Current Biology 24, 652–657, March 17, 2014 ©2014 Elsevier Ltd All rights reserved http://dx.doi.org/10.1016/j.cub.2014.01.041

Report

A Neoproterozoic Transition in the Marine Nitrogen Cycle

Patricia Sánchez-Baracaldo,[1,2,*] Andy Ridgwell,[2] and John A. Raven[3,4]

[1]School of Biological Sciences, University of Bristol, Woodland Road, Bristol BS8 1UG, UK

[2]School of Geographical Sciences, University of Bristol, Bristol BS8 1SS, UK

[3]Division of Plant Science, University of Dundee at the James Hutton Institute, Invergowrie, Dundee DD2 5DA, UK

[4]School of Plant Biology, University of Western Australia, Crawley, WA 6009, Australia

Summary

The Neoproterozoic (1000–542 million years ago, Mya) was characterized by profound global environmental and evolutionary changes, not least of which included a major rise in atmospheric oxygen concentrations [1, 2], extreme climatic fluctuations and global-scale glaciation [3], and the emergence of metazoan life in the oceans [4, 5]. We present here phylogenomic (135 proteins and two ribosomal RNAs, SSU and LSU) and relaxed molecular clock (SSU, LSU, and *rpoC1*) analyses that identify this interval as a key transition in the marine nitrogen cycle. Specifically, we identify the Cryogenian (850–635 Mya) as heralding the first appearance of both marine planktonic unicellular nitrogen-fixing cyanobacteria and non-nitrogen-fixing picocyanobacteria (*Synechococcus* and *Prochlorococcus* [6]). Our findings are consistent with the existence of open-ocean environmental conditions earlier in the Proterozoic adverse to nitrogen-fixers and their evolution—specifically, insufficient availability of molybdenum and vanadium, elements essential to the production of high-yielding nitrogenases. As these elements became more abundant during the Cryogenian [7, 8], both nitrogen-fixing cyanobacteria and planktonic picocyanobacteria diversified. The subsequent emergence of a strong biological pump in the ocean implied by our evolutionary reconstruction may help in explaining increased oxygenation of the Earth's surface at this time, as well as tendency for glaciation.

Results and Discussion

Phylogenomic Analyses Addressing the Evolution of Nitrogen-Fixing Planktonic Cyanobacteria

While recent phylogenomic and trait evolution studies [9, 10] have shown that early cyanobacteria lineages were already able to fix nitrogen (N) in freshwater environments, the timing of appearance of marine planktonic N-fixing cyanobacteria is still unclear. These microorganisms exert a primary control on the productivity of the modern marine biosphere by providing biologically available ammonium to the open ocean [11], with the implication that the carbon cycle would have operated rather differently prior to their proliferation in the open ocean. By implementing phylogenomic and Bayesian relaxed molecular clock analyses, we estimate the phylogeny and age divergences of planktonic marine N-fixing cyanobacteria (including *Crocosphaera*, *Cyanothece*, cyanobacterium UCYN-A, and *Trichodesmium*). We identify the Neoproterozoic (1,000–541 million years ago, Mya) as the interval when the ancestors of today's main contributors to the N cycle apparently first evolved and diversified in marine environments, and thus when a substantial inventory of fixed nitrogen in the ocean could first have been established. We also identify an origin consistently postdating the appearance of unicellular N-fixers for the non-N-fixing marine *Synechococcus* and *Prochlorococcus* (*SynPro*) clade, which represents some of the most abundant photosynthetic organisms on Earth today.

We performed phylogenetic analyses in two stages. First, we generated genome analyses from 69 cyanobacteria genomes to determine the deep-branching relationships of cyanobacteria. From these analyses, we obtained two possible evolutionary scenarios (see Figures S1 and S2 available online) congruent with previous phylogenomic studies [9, 10, 12], to which we added a third alternative genomic topology [6]. All three scenarios were later implemented as genome constraints/topologies: (1) SATé (Figure S1) [9, 10], (2) RAxML (Figure S2) [12], and (3) Blank and Sánchez-Baracaldo [6]. Because there are still discrepancies among phylogenomic analyses determining the position of *Synechococcus elongatus* and the LPP clade (containing *Leptolyngbya*, *Plectonema*, *Phormidium*, and *Synechococcus* PCC7335) [6, 9, 10, 12, 13], we evaluated whether different evolutionary scenarios (genome topologies) have any influence when estimating ages for planktonic N-fixing cyanobacteria and the marine *SynPro* clade. Second, we achieved a broader taxonomic sampling including 126 taxa by analyzing nucleotide data (SSU, LSU, and *rpoC1*) while enforcing the three backbone genome constraints. This data set included close relatives of planktonic N-fixing cyanobacteria for which genomes are not yet available (e.g., *Hydrocoleum* and *Blennothrix*; Figure 1). Interestingly, *Trichodesmium*'s closest relatives are found in marine littorals, and *Crocosphaera* relatives are found in freshwater environments.

Relaxed molecular clock analyses were performed on a nucleotide data set (SSU, LSU and *rpoC1*) using a Bayesian approach [14, 15] and three fossil calibration constraints [6]. Bayes factor analyses favored the independent-rates model over the autocorrelated-rates model [16]. This might be due to the great variation in inherited factors at very large temporal scales [15] and sharp shifts in evolutionary rates associated with changes in life history in the evolution of the *SynPro* clade as they adapted to oligotrophic environments [17]. Analyses indicate that planktonic marine N-fixing cyanobacteria and the marine *SynPro* appeared during the Neoproterozoic or early Cambrian (542–485 Mya) [6]. Age estimates across all analyses are summarized in Tables 1 and S1 and Figures 1, S3, and S4 and are in broad agreement.

We identify the appearance of the unicellular N-fixing cyanobacteria in the surface ocean (*Crocosphaera* and relatives) during the Neoproterozoic (Figures 1, S3, and S4). Median age estimates for the common ancestor of this marine group (node 2) range between 932 and 665 Mya. Most analyses show that that the common ancestor of the marine picocyanobacteria (node 7) appeared slightly later during the Cryogenian (823–644 Mya). A common ancestor for *Prochlorococcus* (node 8) was estimated to have appeared between 684 and

*Correspondence: p.sanchez-baracaldo@bristol.ac.uk

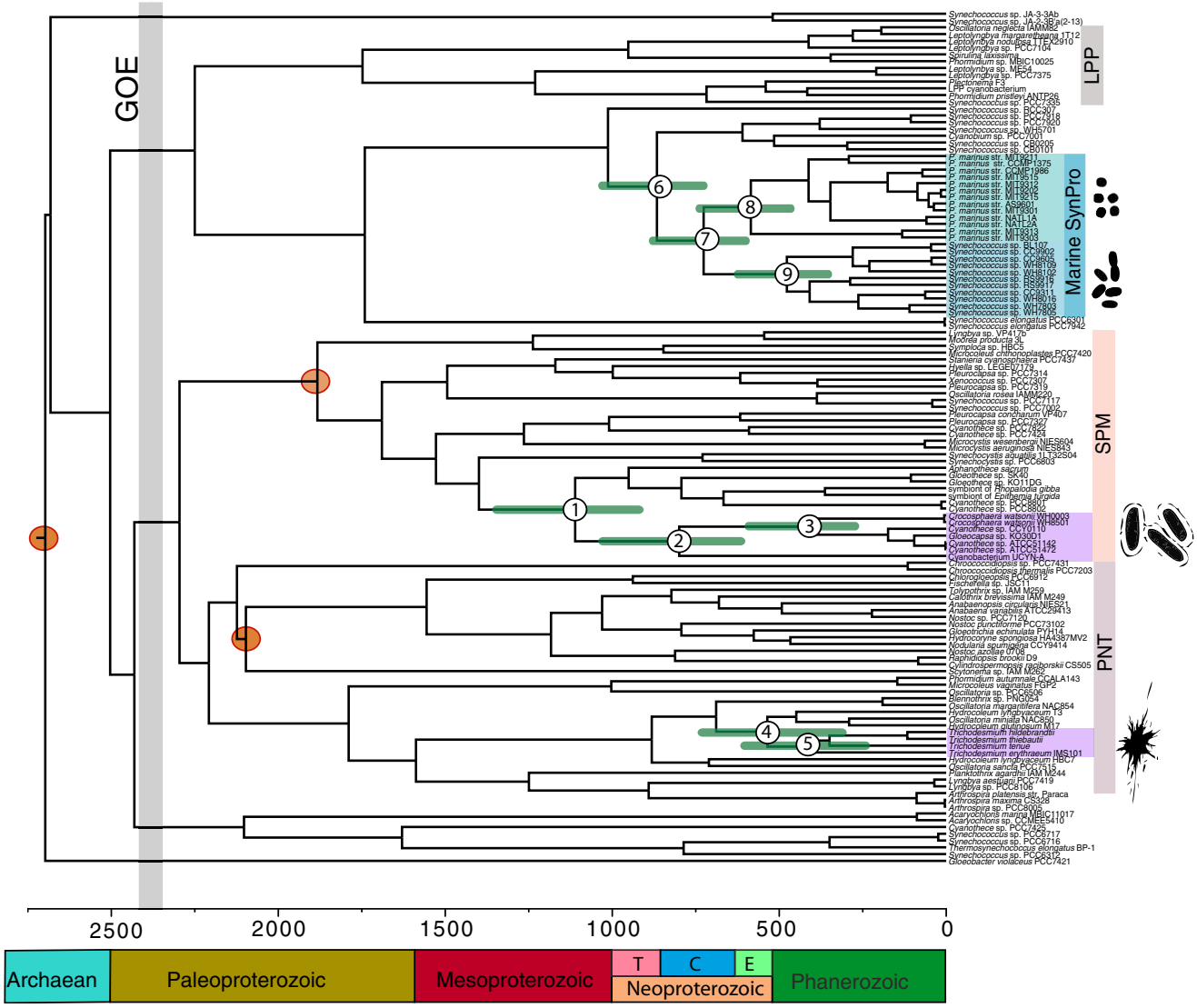

Figure 1. The Origin and Diversification of Cyanobacteria as Inferred from Geologic and Genomic Data

The phylogenetic tree was estimated in a two-step process. First, a genome tree with 69 taxa was generated using 135 proteins and two ribosomal RNAs (SSU and LSU). Second, a broader taxa sampling was achieved for an additional data set by using SSU, LSU, and *rpoC1*, enforcing genome constraint 2 (RAxML) [9, 10]. Bayesian relaxed molecular clock analyses were implemented using MCMCtree (based on SSU, LSU, and *rpoC1*) to estimate divergence times. Three calibrations (brown circles) were used [6] for the tree shown and were treated as soft bounds in different experimental settings. The root of the tree was set at 2.7 giga-annum. Numbered nodes 1–9 indicate divergence times for planktonic N-fixers and marine *SynPro* nodes. Green bars represent the posterior 95% confidence intervals for the node ages; values are given in Table 1.

543 Mya, and for marine *Synechococcus* between 550 and 421 Mya. Finally, planktonic filamentous N-fixers, *Trichodesmium*, diverged from their close benthic relatives between 609 and 500 Mya. The age estimates for ancestral nodes of planktonic unicellular N-fixing cyanobacteria and marine *SynPro* [6] are summarized in Table 1.

N-Fixing Cyanobacteria and the Geological Record

Nitrogen is an essential nutrient whose availability limits the productivity of the biosphere [18]. The availability of fixed nitrogen in the ocean is primarily regulated by the balance between (1) N fixation, whereby N is converted from generally biologically inaccessible N_2 to highly bioavailable ammonium (NH_4^+) (subsequently to nitrate), and (2) losses through denitrification, which while encompassing several different pathways effectively accomplishes the reverse transformation. Although fixed nitrogen is also derived via rivers and dust from terrestrial ecosystems as well as via lightning [18], biological fixation by cyanobacteria near the ocean surface dominates the supply of fixed nitrogen to the open ocean. The importance of N-fixing cyanobacteria would have been even greater during intervals of the geological past when widespread anoxia enhanced the rate of denitrification and hence loss of fixed nitrogen [19]. Prior to the appearance of the major groups of N-fixing cyanobacteria that dominate the modern open ocean (unicellular *Crocosphaera* and relatives of *Cyanothece*, filamentous non-heterocyst-forming *Trichodesmium*, and symbionts within unicellular eukaryotic algae), the marine biosphere would thus have very likely been N limited [20].

Table 1. Posterior Age Estimates in Million Years

	Root Age	Node ID 1	2	3	4	5	6	7	8	9
MCMCtree										
GC1	3,000	1,300 (1,055, 1,546)	932 (688, 1,198)	468 (307, 669)	593 (408, 821)	458 (282, 674)	977 (795, 1,189)	818 (657, 1,008)	656 (518, 826)	534 (393, 710)
	2,700	1,047 (830, 1,290)	782 (542, 1,041)	343 (201, 530)	609 (394, 881)	424 (214, 679)	884 (696, 1,112)	758 (589, 966)	625 (483, 797)	480 (338, 660)
	2,500	1,025 (817, 1,244)	767 (529, 1,019)	335 (195, 525)	593 (378, 856)	410 (202, 669)	860 (676, 1,078)	736 (568, 943)	602 (451, 779)	473 (332, 661)
GC2	3,000	1,299 (1,052, 1,542)	931 (682, 1,204)	467 (305, 670)	594 (407, 830)	501 (407, 830)	977 (800, 1,189)	823 (823, 1,013)	660 (524, 826)	537 (368, 713)
	2,700	1,111 (904, 1,356)	800 (587, 1,046)	409 (265, 588)	536 (372, 741)	411 (252, 607)	866 (711, 1,050)	726 (589, 892)	585 (468, 736)	477 (351, 635)
	2,500	1,068 (877, 1,263)	770 (563, 990)	394 (258, 568)	511 (351, 706)	394 (241, 582)	821 (675, 995)	682 (556,839)	543 (433,685)	451 (334,599)
GC3	3,000	1,162 (925, 1,456)	836 (594, 1,115)	434 (279, 642)	600 (399, 863)	449 (261, 695)	1,026 (817, 1,315)	850 (674, 1,099)	684 (525, 894)	550 (390, 759)
	2,700	1,079 (879, 1,287)	776 (556, 1,009)	404 (252, 589)	569 (375, 814)	425 (242, 653)	948 (759, 1,182)	785 (627, 987)	631 (488, 807)	514 (369, 689)
	2,500	1,049 (851, 1,254)	751 (538, 982)	389 (243, 574)	552 (367, 794)	411 (230, 638)	914 (723, 1,154)	754 (592, 956)	604 (468, 769)	495 (352, 673)
BEAST										
	3,000	1,007 (852, 1,163)	691 (519, 879)	330 (221, 461)	512 (369, 669)	371 (230, 513)	804 (671, 950)	671 (561, 709)	558 (455, 678)	437 (336, 548)
	2,700	965 (812, 1,117)	665 (500, 835)	312 (205, 430)	500 (359, 651)	362 (235, 515)	776 (641, 926)	644 (523, 769)	545 (437, 664)	421 (322, 538)
	2,500	991 (837, 1,157)	690 (516, 871)	344 (222, 485)	552 (400, 747)	399 (241, 576)	875 (711, 1,070)	727 (587, 899)	593 (472, 744)	496 (370, 641)

Node IDs correspond to those shown in Figure 1. MCMCtree age estimates are given for analyses under the independent-rates model [15]. Genome constraint 1 (GC1): SATé [9, 10]; genome constraint 2: RAxML [12]; genome constraint 3: Blank and Sánchez-Baracaldo [6]. Three separate analyses were performed, setting the root at a maximum age of 3,000 mega-annum (Ma), 2,700 Ma, and 2,500 Ma. BEAST age estimates are given for analyses under uncorrelated log-normal rate distribution (UCLN) [15]. Three independent analyses were carried out, adjusting 95% of the root prior distribution to reflect the maximum ages used above. Values in parenthesis correspond to posterior 95% confidence intervals associated with median age estimate.

Recent geochemical evidence suggests that oxygenic photosynthesis, and by implication the first appearance of cyanobacteria in any environment, could have occurred as far back as 3,000 Mya (3 billion years ago, Gya) [21]. Phylogenetic reconstructions and trait analyses [6] indicate that cyanobacteria started to move from their origin in freshwater ecosystems to start to diversify in coastal brackish and marine environments rather later—around 2.4 Gya, at a time closely coincident with multiple lines of evidence for a step increase in the oxygenation of the Earth's surface at the "Great Oxygenation Event" in the early Paleoproterozoic [22, 23] (Figure 2). An interval of more than one billion years then separates the first possible appearance of marine cyanobacteria from the diversification and widespread colonization of marine planktonic environments during the Neoproterozoic that we reconstruct here (Figure 2, stage II). Much of this interval, as evidenced by late Paleoproterozoic through early- to mid-Mesoproterozoic carbon isotope variability, has previously been interpreted as reflecting relatively stable global environmental conditions and geobiological quiescence. What was the relationship between life and environment during this time—did an evolutionary hiatus among N-fixing organisms hold up further oxidation of the biosphere, did the environmental conditions prevailing in the open ocean preclude progressive evolutionary development [1], or both?

The apparent delay in the evolutionary transition in marine N cycling is consistent with changing patterns of trace element availability [7]. Molybdenum (Mo) is a potentially limiting trace nutrient and moreover is an essential constituent of the dominant N_2-fixing nitrogenase enzyme complex [24]. Although highly soluble in modern oxic ocean conditions, Mo is efficiently scavenged in sulfidic (free H_2S) conditions [7, 25]. Mo concentrations are thought to have been sufficiently low during much of the Proterozoic [2] to be limiting to open-ocean N-fixers and drive the open ocean toward N limitation and oligotrophy [26] (Figure 3). Here we suggest that the necessary diversity and hence capacity for substantive global rates of N fixation also did not exist at this time because a weakly productive and Mo-limited ocean also limited the evolutionary development and diversification of N-fixers.

It should be recognized that marine productivity need not have been low away from the open ocean, and that the ocean would not have been barren during the late Proterozoic through Mesozoic. Freshwater and coastal environments close to riverine sources of solubilized Mo would have supported a community of N-fixers adapted to less saline and/or benthic environments. Ocean margin environments would have been productive and supported an active N cycle during the Mesoproterozoic [27]. An active carbon cycle existing at the margins would account for the occurrence of organic carbon-rich sediments ("black shales") (e.g., Scott et al. [1]) as well as creating the source of H_2S needed to scavenge Mo from the open ocean. A limited degree of carbon fixation in the open ocean itself could also have been supported by the leaking of ammonium from the margins as well as by anoxygenic photolithotrophic bacteria, some of which are N-fixers [28, 29].

Understanding why a state of Mo limitation in the open ocean generally persisted throughout the late Paleoproterozoic and Mesozoic is complicated because organic matter production and subsequent degradation via sulfate reduction are required to generate free H_2S and hence scavenge dissolved Mo from the water column (Figure 3). This implies

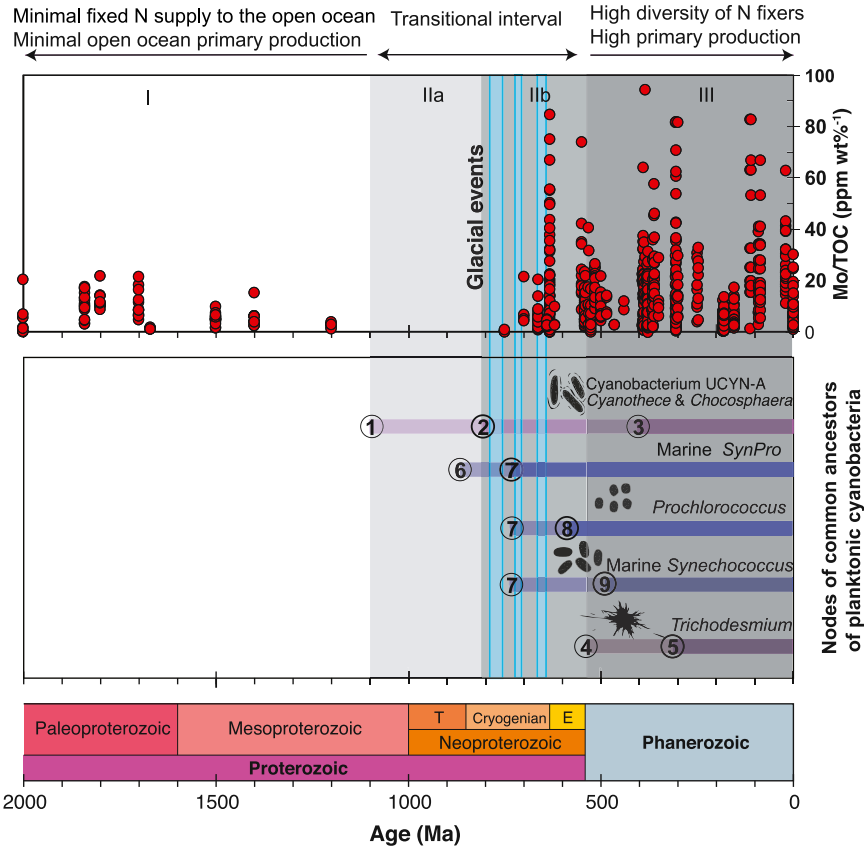

Figure 2. Age Estimates for Marine Planktonic Cyanobacteria and Temporal Trends in Molybdenum Enrichment

Temporal correspondence between records of changing molybdenum (Mo) enrichment in black shales (top panel), an indicator of the oceanic Mo inventory [1, 2], and age divergence for planktonic N-fixing cyanobacteria and the marine *SynPro* clades (bottom panel), with the nodes corresponding to those in Figure 1 and Table 1. The relative timing of occurrences of extreme glaciation is illustrated by vertical blue highlights. Three stages of the potential for marine N cycling and primary production become apparent: stage I corresponds to a virtually barren ocean, stage III corresponds to a modern-like productive ocean with a diverse community of N-fixers, and stages IIa and IIb reflect a two-stage transition between these two very different Earth system states.

that a negative feedback must have existed in the marine system, keeping N fixation and hence productivity low, but not so low as to shut off the supply of new H_2S completely. Oceanic Mo concentrations could hence have been regulated at concentrations low enough to limit further evolution among N-fixers. Although alternative nitrogenases exist, Fe-Mo nitrogenase appears to be the most efficient in N_2 binding [24], suggesting that substituting e.g. Fe-Fe would not greatly strengthen the N cycle and could not produce an alternative evolutionary pathway to high open-ocean productivity. However, terrestrial weathering and with it the supply of Mo would have been extremely high in the greenhouse aftermath of Neoproterozoic glaciation [30, 31], which might have provided a possible trigger for escaping the feedback.

Observations of increasing Mo enrichment in black shales and the onset of nonlimiting Mo concentrations in the open ocean during the Cryogenian [1, 2, 8] coincide with our age estimations of planktonic N-fixing cyanobacteria in marine environments (Figure 2, stage III). The closely coincident origin of other phytoplankton such as *SynPro* (Figure 1) [6] as well as an increasing contribution and diversification of eukaryotic phytoplankton [32–34] is consistent with the spread of unicellular N-fixing cyanobacteria to the open ocean and a substantive increase in the strength of the ocean's biological pump. In turn, changes in nitrogen and carbon cycling are likely to have played an important role through increased organic matter burial in marine sediments and atmospheric pCO_2 drawdown due to increased biological export to the ocean floor [35]. Increased oxygen availability as a result of increased carbon burial might then have enabled the transition to a high Mo/low H_2S state of the ocean.

Conclusions

Recent advances in proxies and sampling of the geological record have highlighted the Neoproterozoic as an interval of profound global environmental change. However, in light of the multiple covarying environmental changes and complex web of potential positive and negative feedbacks, refining key geochemical and biological proxies of marine environmental conditions alone is insufficient. More effective linking with evolutionary analyses and phylogenetic reconstructions will be essential if we are to unravel cause and effect in the events surrounding the emergence of complex life in the oceans. Our phylogenomic analysis now adds the evolutionary establishment of the capacity for a strong marine N cycle in the open ocean to the changes occurring at this time. Considering that the marine *SynPro* clade represents some of the most abundant photosynthetic organisms in the modern ocean [17, 36], their appearance, quite possibly linked to a step increase in the availability of fixed nitrogen, would have had a major impact on rates of production of organic matter in the open ocean. A more integrated geochemical- phylogenetic approach could also help unravel the causes and consequences of perturbations of global carbon cycling (the Lomagundi-Jatuli carbon isotopic event [37]) and the first major rise in atmospheric oxygen near the start of the Proterozoic.

Experimental Procedures

Data Sets and Phylogenies

Sequences from 69 cyanobacterial genomes representing taxa from all well-supported monophyletic groups described previously [6, 9, 10, 12] were included in this study. The 135 proteins and ribosomal RNAs (SSU and LSU) analyzed are highly conserved and have undergone a minimum number of gene duplications [6]. A broader taxonomic sampling (with a total of 126 taxa) was implemented to include close relatives of planktonic N-fixing cyanobacteria and other underrepresented groups in the genomic data set. Maximum-likelihood analyses were performed in RAxMLGUI v1.1 [38], and Bayesian analyses were performed in MrBayes v3.2.1 [39]. Accession numbers for all taxa were obtained from GenBank or using Geneious 5.5.6 and are listed in Tables S2 and S3.

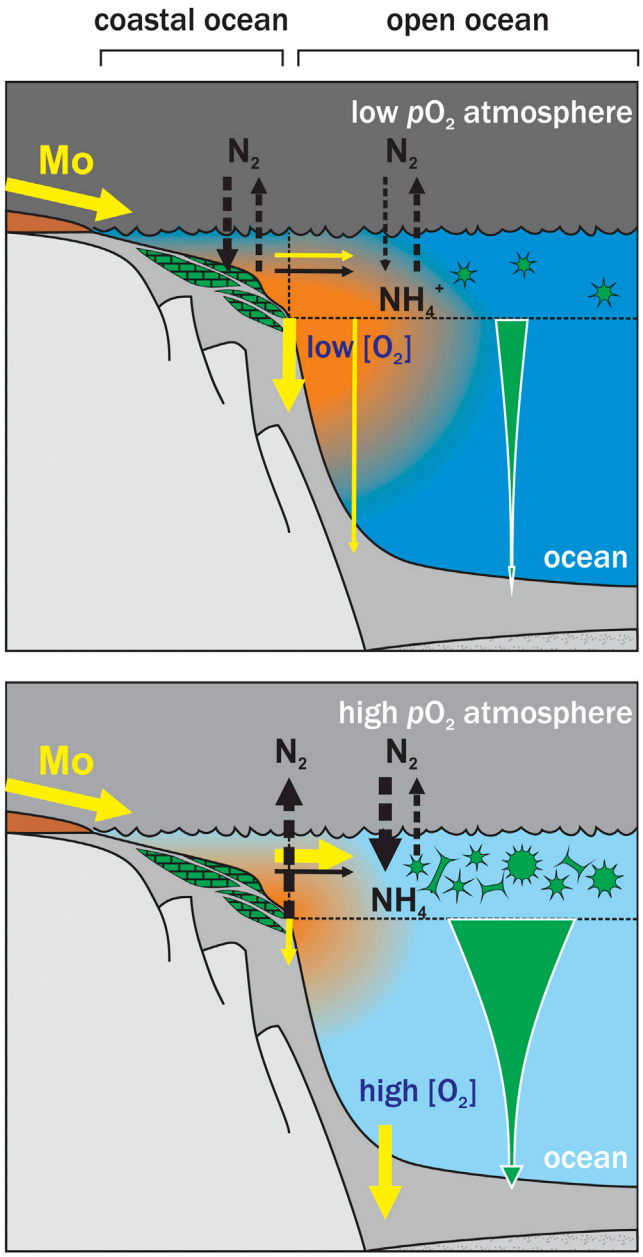

Figure 3. Relationship between Marine Nitrogen Cycling and Molybdenum

Illustration of potential relationship between molybdenum (Mo) and nitrogen (N) cycles prior to (top) and following (bottom) the evolution of a diverse community of N-fixers in the open ocean and greater oxygenation of the biosphere. In a low-oxygen environment, areas of sulfidic conditions (orange) would have been much more extensive than in the modern ocean, and scavenging of Mo by reaction with H_2S would have been efficient and the dominant sink of Mo in the ocean. The restricted supply of Mo to the open ocean would have limited N fixation and also the diversity of the N-fixing community. In a higher-oxygen environment with restricted zones of low $[O_2]$ and sulfidic conditions in the ocean, Mo supply to the open ocean would have been much greater and much less efficiently removed onto ferromanganese crusts at the seafloor. Sedimentary rather than water column denitrification would have represented the dominant loss of fixed nitrogen (e.g., NH_4^+) to N_2, but high concentrations of Mo in the open ocean would have supported a diverse and N-productive community.

Bayesian Divergence Time Estimation

We performed Bayesian relaxed molecular clock analyses by implementing MCMCtree [14] and BEAST v1.7.5 [40] to estimate divergence times (Table 1). Bayes factors were estimated in the program Tracer v1.5.0 using values from MCMCtree analyses, and these favored the independent-rates model over the autocorrelated-rates model (see Nylander et al. [16]). Age estimates implementing both models in MCMCtree are shown in Tables 1 and S1. Three evolutionary hypotheses were evaluated as described above [6, 9, 10, 12]. For all age calibrations, both minimum and maximum bounds were soft and specified by uniform distributions between the maximum and minimum time constraints with 2.5% tail probabilities above and below these limits, allowing for molecular data to correct for conflicting fossil information. In BEAST, we applied relaxed clocks with uncorrelated log-normal rate distribution (UCLN; Table 1) and set monophyly constrains for the main monophyletic groups based on the topology shown in Figure 1.

Fossil Constraints

We used age constraints recently implemented in studies of cyanobacteria [6]. The maximum and minimum ages implemented here refer to accepted ages for the origin of oxygenic photosynthesis in the literature. Experiments reported here were performed with three different maximum ages for the cyanobacterial root: 2.5 giga-annum (Ga) [41], 2.7 Ga [42], and 3.0 Ga [21]. The minimum age for the cyanobacterial root was set at 2.32 Ga [22].

For the Nostocales, a minimum age of 2.1 Ga was used because nostocalean akinete (a spore-like structure) microfossils first appeared around this time [43, 44]. It has been proposed that the presence of free oxygen selected for the appearance of akinetes [44]. For the Pleurocapsales, a minimum age was set at 1.7 Ga based on first appearance of their microfossils [45]. A maximum age of 2.45 Ga was chosen for these two groups because their ancestors were estimated to have large cell diameters via ancestral character state reconstruction analyses [6].

A more detailed description of the methodology is found in the Supplemental Experimental Procedures.

Supplemental Information

Supplemental Information includes four figures, three tables, and Supplemental Experimental Procedures and can be found with this article online at http://dx.doi.org/10.1016/j.cub.2014.01.041.

Acknowledgments

We thank C.E. Blank and F. Monteiro for formative discussions; R. Warnock and G. Thomas for assistance with the analyses; and E.J. Stone, S. Greene, and J. Huelsenbeck for constructive comments. BEAST analyses were performed at the High Performance Computer facility (BlueCrystal 3) at University of Bristol. Funding support for this work came from a Royal Society Dorothy Hodgkin Fellowship to P.S.-B. and a Royal Society University Research Fellowship to A.R. The University of Dundee is a registered Scottish charity, No. SC015096.

Received: June 25, 2013
Revised: October 21, 2013
Accepted: January 17, 2014
Published: February 27, 2014

References

1. Scott, C., Lyons, T.W., Bekker, A., Shen, Y., Poulton, S.W., Chu, X., and Anbar, A.D. (2008). Tracing the stepwise oxygenation of the Proterozoic ocean. Nature *452*, 456–459.
2. Sahoo, S.K., Planavsky, N.J., Kendall, B., Wang, X., Shi, X., Scott, C., Anbar, A.D., Lyons, T.W., and Jiang, G. (2012). Ocean oxygenation in the wake of the Marinoan glaciation. Nature *489*, 546–549.
3. Fairchild, I.J., and Kennedy, M.J. (2007). Neoproterozoic glaciation in the Earth System. J. Geol. Soc. London *164*, 895–921.
4. Yuan, X., Chen, Z., Xiao, S., Zhou, C., and Hua, H. (2011). An early Ediacaran assemblage of macroscopic and morphologically differentiated eukaryotes. Nature *470*, 390–393.
5. Erwin, D.H., Laflamme, M., Tweedt, S.M., Sperling, E.A., Pisani, D., and Peterson, K.J. (2011). The Cambrian conundrum: early divergence and later ecological success in the early history of animals. Science *334*, 1091–1097.
6. Blank, C.E., and Sánchez-Baracaldo, P. (2010). Timing of morphological and ecological innovations in the cyanobacteria—a key to understanding the rise in atmospheric oxygen. Geobiology *8*, 1–23.

7. Anbar, A.D., and Knoll, A.H. (2002). Proterozoic ocean chemistry and evolution: a bioinorganic bridge? Science *297*, 1137–1142.
8. Reinhard, C.T., Planavsky, N.J., Robbins, L.J., Partin, C.A., Gill, B.C., Lalonde, S.V., Bekker, A., Konhauser, K.O., and Lyons, T.W. (2013). Proterozoic ocean redox and biogeochemical stasis. Proc. Natl. Acad. Sci. USA *110*, 5357–5362.
9. Larsson, J., Nylander, J.A., and Bergman, B. (2011). Genome fluctuations in cyanobacteria reflect evolutionary, developmental and adaptive traits. BMC Evol. Biol. *11*, 187.
10. Latysheva, N., Junker, V.L., Palmer, W.J., Codd, G.A., and Barker, D. (2012). The evolution of nitrogen fixation in cyanobacteria. Bioinformatics *28*, 603–606.
11. Zehr, J.P., and Kudela, R.M. (2011). Nitrogen cycle of the open ocean: from genes to ecosystems. Annu. Rev. Mar. Sci. *3*, 197–225.
12. Shih, P.M., Wu, D., Latifi, A., Axen, S.D., Fewer, D.P., Talla, E., Calteau, A., Cai, F., Tandeau de Marsac, N., Rippka, R., et al. (2013). Improving the coverage of the cyanobacterial phylum using diversity-driven genome sequencing. Proc. Natl. Acad. Sci. USA *110*, 1053–1058.
13. Sánchez-Baracaldo, P., Hayes, P.K., and Blank, C.E. (2005). Morphological and habitat evolution in the Cyanobacteria using a compartmentalization approach. Geobiology *3*, 145–165.
14. Yang, Z. (2007). PAML 4: phylogenetic analysis by maximum likelihood. Mol. Biol. Evol. *24*, 1586–1591.
15. Drummond, A.J., Ho, S.Y.W., Phillips, M.J., and Rambaut, A. (2006). Relaxed phylogenetics and dating with confidence. PLoS Biol. *4*, e88.
16. Nylander, J.A.A., Ronquist, F., Huelsenbeck, J.P., and Nieves-Aldrey, J.L. (2004). Bayesian phylogenetic analysis of combined data. Syst. Biol. *53*, 47–67.
17. Scanlan, D.J., Ostrowski, M., Mazard, S., Dufresne, A., Garczarek, L., Hess, W.R., Post, A.F., Hagemann, M., Paulsen, I., and Partensky, F. (2009). Ecological genomics of marine picocyanobacteria. Microbiol. Mol. Biol. Rev. *73*, 249–299.
18. Gruber, N., and Galloway, J.N. (2008). An Earth-system perspective of the global nitrogen cycle. Nature *451*, 293–296.
19. Monteiro, F.M., Pancost, R.D., and Ridgwell, A. (2012). Nutrients as the dominant control on the spread of anoxia and euxinia across the Cenomanian-Turonian oceanic anoxic event (OAE2): Model-data comparison. Paleoceanography *27*, 2012.
20. Falkowski, P.G. (1997). Evolution of the nitrogen cycle and its influence on the biological sequestration of CO_2 in the ocean. Nature *387*, 272–275.
21. Crowe, S.A., Døssing, L.N., Beukes, N.J., Bau, M., Kruger, S.J., Frei, R., and Canfield, D.E. (2013). Atmospheric oxygenation three billion years ago. Nature *501*, 535–538.
22. Bekker, A., Holland, H.D., Wang, P.-L., Rumble, D., 3rd, Stein, H.J., Hannah, J.L., Coetzee, L.L., and Beukes, N.J. (2004). Dating the rise of atmospheric oxygen. Nature *427*, 117–120.
23. Holland, H.D. (2006). The oxygenation of the atmosphere and oceans. Philos. Trans. R. Soc. Lond. B Biol. Sci. *361*, 903–915.
24. Zerkle, A.L., House, C.H., Cox, R.P., and Canfield, D.E. (2006). Metal limitation of cyanobacterial N2 fixation and implications for the Precambrian nitrogen cycle. Geobiology *4*, 285–297.
25. Lyons, T.W., Anbar, A.D., Severmann, S., Scott, C., and Gill, B.C. (2009). Tracking Euxinia in the Ancient Ocean: A multiproxy perspective and Proterozoic case study. Annu. Rev. Earth Planet. Sci. *37*, 507–534.
26. Fennel, K. (2005). The co-evolution of the nitrogen, carbon and oxygen cycles in the Proterozoic ocean. Am. J. Sci. *305*, 526–545.
27. Stüeken, E.E. (2013). A test of the nitrogen-limitation hypothesis for retarded eukaryote radiation: Nitrogen isotopes across a Mesoproterozoic basinal profile. Geochim. Cosmochim. Acta *120*, 121–139.
28. Kharecha, P., Kasting, J., and Siefert, J. (2005). A coupled atmosphere-ecosystem model of the early Archean Earth. Geobiology *3*, 53–76.
29. Canfield, D.E., Rosing, M.T., and Bjerrum, C. (2006). Early anaerobic metabolisms. Philos. Trans. R. Soc. Lond. B Biol. Sci. *361*, 1819–1834, discussion 1835–1836.
30. Hoffman, P.F., and Schrag, D.P. (2002). The snowball Earth hypothesis: testing the limits of global change. Terra Nova *14*, 129–155.
31. Mills, B., Watson, A.J., Goldblatt, C., Boyle, R., and Lenton, T.M. (2011). Timing of Neoproterozoic glaciations linked to transport-limited global weathering. Nat. Geosci. *4*, 861–864.
32. Butterfield, N.J. (1997). Plankton ecology and the Proterozoic-Phanerozoic transition. Paleobiology *23*, 247–262.
33. Kodner, R.B., Pearson, A., Summons, R.E., and Knoll, A.H. (2008). Sterols in red and green algae: quantification, phylogeny, and relevance for the interpretation of geologic steranes. Geobiology *6*, 411–420.
34. Raven, J.A. (2012). Algal biogeography: metagenomics shows distribution of a picoplanktonic pelagophyte. Curr. Biol. *22*, R682–R683.
35. Tziperman, E., Halevy, I., Johnston, D.T., Knoll, A.H., and Schrag, D.P. (2011). Biologically induced initiation of Neoproterozoic snowball-Earth events. Proc. Natl. Acad. Sci. USA *108*, 15091–15096.
36. Johnson, Z.I., Zinser, E.R., Coe, A., McNulty, N.P., Woodward, E.M.S., and Chisholm, S.W. (2006). Niche partitioning among *Prochlorococcus* ecotypes along ocean-scale environmental gradients. Science *311*, 1737–1740.
37. Melezhik, V.A., Huhma, H., Condon, D.J., and Fallick, A.E. (2007). Temporal constraints on the Paleoproterozoic Lomagundi-Jatuli carbon isotopic event. Geology *35*, 655–658.
38. Silvestro, D., and Michalak, I. (2011). raxmlGUI: a graphical front-end for RAxML. Org. Divers. Evol. *12*, 335–337.
39. Ronquist, F., and Huelsenbeck, J.P. (2003). MrBayes 3: Bayesian phylogenetic inference under mixed models. Bioinformatics *19*, 1572–1574.
40. Drummond, A.J., Suchard, M.A., Xie, D., and Rambaut, A. (2012). Bayesian phylogenetics with BEAUti and the BEAST 1.7. Mol. Biol. Evol. *29*, 1969–1973.
41. Rasmussen, B., Fletcher, I.R., Brocks, J.J., and Kilburn, M.R. (2008). Reassessing the first appearance of eukaryotes and cyanobacteria. Nature *455*, 1101–1104.
42. Brocks, J.J., Buick, R., Summons, R.E., and Logan, G.A. (2003). A reconstruction of Archean biological diversity based on molecular fossils from the 2.78 to 2.45 billion-year-old Mount Bruce Supergroup, Hamersley Basin, Western Australia. Geochim. Cosmochim. Acta *67*, 4321–4335.
43. Golubic, S., Sergeev, V.N., and Knoll, A.H. (1995). Mesoproterozoic Archaeoellipsoides: akinetes of heterocystous cyanobacteria. Lethaia *28*, 285–298.
44. Tomitani, A., Knoll, A.H., Cavanaugh, C.M., and Ohno, T. (2006). The evolutionary diversification of cyanobacteria: molecular-phylogenetic and paleontological perspectives. Proc. Natl. Acad. Sci. USA *103*, 5442–5447.
45. Zhang, Y., and Golubic, S. (1987). Endolithic microfossils (cyanophyta) from early Proterozoic stromatolites, Hebei, China. Acta Micropaleontol. Sin. *4*, 1–3.